Computers and Geotechnics 38 (2011) 659–668

Contents lists available at ScienceDirect

Computers and Geotechnics

journal homepage: www.elsevier.com/locate/compgeo

Numerical analysis of soilbags under compression and cyclic shear

Yousef Ansari [a,*], Richard Merifield [a], Haruyuki Yamamoto [b], Daichao Sheng [a]

[a] Centre for Geotechnical and Materials Modelling, The University of Newcastle, Callaghan NSW 2308, Australia
[b] Graduate School for International Development and Cooperation, Hiroshima University, 1-5-1 Kagamiyama, Higashi-Hiroshimashi 739-5829, Japan

ARTICLE INFO

Article history:
Received 1 September 2010
Received in revised form 8 February 2011
Accepted 8 February 2011
Available online 8 May 2011

Keywords:
Soilbag
Finite element model
Contact kinematic constraints
Soil-bag interface
Vertical compression
Cyclic shear

ABSTRACT

This paper presents a finite element model for analysing the behaviour of granular material wrapped with polyethylene bags under vertical compression and cyclic shearing. The simple Mohr–Coulomb model is used to represent the soil behaviour. The polyethylene bag is represented by a linear-elastic–perfect-plastic model. The soil-bag interface is modelled with contact constraints. The main purpose of the numerical analysis is to validate the anticipated performance of soilbags under various loading conditions and hence the effectiveness of soilbags as a method of ground improvement.

1. Introduction

Soilbags or sandbags, "Donow"s in Japanese, continue to be used to construct either temporary or permanent structures and are bags filled with granular materials like sand, crushed stone, or recycled concrete. Granular soils wrapped with bags exhibit the typical characteristics of cohesive-frictional materials [11]. The significant increase in the compression strength of these soilbags has encouraged geotechnical engineers to consider soilbags as a cheap, environmental friendly and convenient alternative for soil reinforcement. While the use of soilbags for temporary purposes has been established for a long time, their use in permanent construction works through quality-controlled soilbags (Solpack) is rather new.

Previous research on the application of solpacks have reported their use as reinforcement for increasing the bearing capacity of soft soil foundations [10,11], as damping layers for the vibration reduction transmitted from traffic loads [9], as facings installed in front of geosynthetic-reinforced soil retaining walls [24], and as ballast foundations of railway tracks for access roads in mountainous areas. More recently, soilbags, due to their significant compressive strength, have been used successfully to construct arch structures to support embankments [3]. Soilbags have already been used to reinforce truck roads in Nagoya City, Japan, with asphalt & concrete pavements or as reinforcement for soft building foundations to improve the bearing capacity of footings as well as to reduce traffic-induced vibrations [7,10]. Other field applications include frost heave prevention [22] in the Hokkaido area, Japan.

The mechanical behaviour of a single soilbag under vertical compression has been investigated by Matsuoka et al. [11] who also proposed a simplified analytical model. The proposed method was validated through biaxial compression and unconfined compression tests. Several simplifying assumptions were considered in their analysis. These assumptions include cohesionless and weightless filling materials, plane strain condition, frictionless soil-bag interface, and unvarying thickness of the bag due to deformations. Other analytical assumptions also were also applied. For instance, the principal stress ratio of the soil is assumed to follow an exponential function; and the volumetric strain of the soilbag is neglected (based on experimental results).

Friction along the contact surfaces of bags, soilbags with different filling materials, and soilbags lying on different base materials has been experimentally investigated by means of a series of laboratory shear tests [9]. Average initial and peak frictional coefficients for various contact interfaces were obtained. The results show that frictional angle due to horizontal loading of soilbags is dependent on the grain size of the filling material as a result of local angularity. Maximum horizontal resistance of soilbags resting on top of other soilbags is shown to be directly proportional to the inclination angle of that soilbag. It is also illustrated that horizontal sliding resistance of soilbags could significantly be increased by bedding in concrete slabs between soilbags and rockfill base materials.

* Corresponding author. Tel.: +61 450519102.
E-mail address: yousef.ansari@uon.edu.au (Y. Ansari).

0266-352X/$ - see front matter © 2011 Elsevier Ltd. All rights reserved.
doi:10.1016/j.compgeo.2011.02.002

Yamamoto et al. [26] performed some large-deformation laboratory tests on soilbags filled with silica sand. In their studies they introduced an "equivalent damping ratio" which for the assembly of soilbags was much higher than those of both the concrete structures and steel structures by a ratio of 6 and 15, respectively.

Matsuoka and Liu [10] conducted small-deformation laboratory tests on solpacks in order to evaluate their vibration reduction potential along the vertical direction. As a result, layers of soilbags were suggested to be used as vibration absorbers in order to reduce traffic-induced vibrations.

Lohani et al. [6] investigated the effects of soilbag materials, backfill soil type, and number of soilbags on compression strength and shear strength in a soilbag-pile. It was concluded that the initial compaction of soilbags and preloading effectively decrease the creep deformation and favourably increase the initial stiffness of the bags. In addition, results of lateral shear tests revealed that the shear strength of a soilbag pile is substantially smaller compared to its compression strength. Low initial stiffness of virgin soilbags during relatively small compression is introduced as one drawback of soilbag-piles. Subsequently, Matsushima et al. [13] showed that a pile of soilbags is much less stable when sheared laterally than when compressed vertically.

Although numerous studies related to field and laboratory tests on soilbags can be found in the literature, numerical studies of soilbags under different loading circumstances are relatively scarce. This is in part due to the complexities arising from simulating the real geometry of a soilbag plus imposing real soilbag assembly constraints. Nonetheless, numerical analysis can be used to validate the anticipated behaviour of soilbags under complex loading conditions.

In [15], a numerical analysis of the ground reinforced by soilbags has been conducted by applying an elasto-plastic finite element analysis (FEA). The soilbags in the ground are represented by truss elements. Finite deformation is considered in the analysis due to the occurrence of large deformations in the model tests. The numerical results show good agreement with two-dimensional model tests on aluminium rods, both qualitatively and quantitatively. Muramatsu et al. [16] further evaluated the damping effects of soilbags against vibration via numerical simulation. Again, soilbags are represented by truss elements. The model proposed by Nakai and Hinokio [17] was used to represent the soil behaviour. The simulated results seem to verify the effectiveness of soilbags as a vibration damping material. More recently, Tantono and Bauer [23] conducted numerical analysis of a sandbag under vertical compression. They used a hypoplastic model to represent the sand in the bag and a linear-elastic–perfect-plastic model for the bag. The bag is modelled with membrane elements. Frictionless and interlocked interfaces between soil and bag have been considered and the evolution of the tensile force within the bag has been investigated for both scenarios. The numerical results seem to verify the behaviour of soilbags under compression.

In this study, a finite element model is presented for analysing the behaviour of granular material wrapped with polyethylene bags under vertical compression and cyclic shearing. Numerical results are compared with the simplified analytical solutions to assess the compression capacity of soilbags under vertical loads. The energy dissipation potential of soilbags under cyclic shearing is also investigated.

2. Finite element model for soilbag

The behaviour of frictional soil is represented by a non-associated Mohr–Coulomb model. More advanced models could have been used. However, the main purpose of the analysis here is to study the behaviour of a soil-bag assemblage. It is deemed beneficial to investigate what can be achieved with a simple and perhaps most commonly used soil model. The Mohr–Coulomb model has a rounded yield surface on the deviatoric plane using the M(θ) method [2,19]. Again, more advanced models such as the Matsuoka and Nakai [12] or the Lade and Duncan [4] models could be used, but would not lead to significant difference in the numerical results. The Mohr–Coulomb model is implemented in the commercial FEM code ABAQUS and it is a matter of convenience to use this model to represent the behaviour of the frictional material. The bag material is modelled using a linear-elastic–perfect-plastic von Mises model.

2.1. Soil-bag interface

One difficulty in simulating real behaviour is that loads applied to the assembly of a soilbag have to be transferred between soil and bag primarily through contact of surfaces. One possible solution to this intricate loading condition is to use interface or joint elements where a normal and tangential stiffness are used to model the pressure transfer and friction at the interfaces. Such elements can have a very small or even zero thickness, but cannot be used for large interfacial displacements or surface separation and reclosure.

An alternative approach for modelling interfacial contact problems between two solid bodies is to use contact kinematic constraints which take into account nonlinearities due to large deformations, surface separation and reclosure. The application of contact elements for geomechanics problems is described in further detail in Sheng et al. [20,21].

In the finite element analysis in this paper, contact elements are used to model the soil-bag interaction. The simple Coulomb friction law is used to define the friction between the soil and the bag:

$$\begin{aligned} &g_t = 0, \quad \text{when } \mu t_N - |t_T| > 0 \rightarrow (\text{stick state}) \\ &|g_t| > 0, \quad \text{when } \mu t_N - |t_T| = 0 \rightarrow (\text{slip state}) \\ &g_t(\mu t_N - |t_T|) = 0 \end{aligned} \tag{1}$$

where g_t is the relative displacement in the tangential direction at the interface, t_T is the tangential stress at contact, and μ is the coefficient of friction.

Normal forces at contacts are transferred via a simple constraint:

$$\begin{aligned} &g_N = 0, \quad \text{when } t_N > 0 \\ &g_N > 0, \quad \text{when } t_N = 0 \\ &t_N g_N = 0 \end{aligned} \tag{2}$$

where g_N is the relative displacement in the normal direction (or the normal gap), and t_N is the normal stress at the contact.

The normal and tangential gaps are computed from the displacements. The normal and tangential stresses are then related to the normal and tangential gaps, respectively, via the penalty method [25]. The only parameter involved in the contact constraints is the interfacial friction μ.

2.2. Finite element code

There are several commercial packages that can be used to analyse large deformation contact mechanics problems. ABAQUS is one of these codes and it has some reasonable constitutive models for geomaterials. Sheng et al. [18] used 'ABAQUS' to simulate the installation and loading of displacement piles. The corresponding numerical results have been compared with measured values from centrifuge tests. Merifield et al. [14] reported the results of finite element analyses of shallowly embedded pipelines under vertical and horizontal load using 'ABAQUS'.

The problem mainly focuses on the evolution of stress and deformation in a soilbag assembly under monotonic vertical loading and cyclic shear loading conditions. Numerical analyses are carried out for both two-dimensional (2D) and three-dimensional (3D) models. A 3D analysis was necessary in order to model the thin surface of the wrapping material with membrane elements. Both models take into account the contact boundary conditions at the soil-bag interface. Accordingly, large frictional sliding, surface separation and reclosure at the soil-bag interfaces are permitted.

Ordinary polyethylene (PE) bags are considered. In the first scenario, the soilbag is subjected to an unconfined vertical compression while the second scenario deals with the cyclic horizontal shearing of a soilbag.

The wrapping PE material has an initial thickness of 0.1 mm. It is considered as a linear-elastic–perfect-plastic material with the following properties: Young's modulus (E) of 500 MPa, Poisson's ratio (υ) of 0.3, yield stress (σ_y) of 100 MPa. These values are typical for PE bag materials according to Matsuoka and Liu (2006).

The granular material was modelled as a non-associated Mohr–Coulomb material with Young's modulus (E) of 100 MPa, Poisson's ratio (υ) of 0.3, internal friction angle of 40°, dilation angle of 5–15°, and cohesion (c) of 1 kPa. These material properties are typical for dense sands or gravels [5]. The small cohesion is used to avoid numerical instability.

The friction coefficient between the soil and the bag is assumed to be 0.84, which is equivalent to the internal friction angle of the soil ($\tan 40^\circ = 0.84$). The bag and the soil are allowed to separate whenever the contact normal stress becomes negative (tension).

2.3. FE Mesh for soilbag under compression

Three-dimensional and two-dimensional numerical simulation of an 80 cm × 40 cm × 10 cm soilbag under unconfined vertical compression is carried out in order to study the behaviour of the soilbag under a vertical compressive load. To minimize the calculation times, the symmetrical geometry of the soilbag is used and accordingly, only a quarter of the soilbag is modelled. The finite element meshes for the assembly of a soilbag are shown in Fig. 1. The assembly consists of a rigid loading panel, the wrapping bag and the soil inside (Fig. 2). The rigid loading panel is used to ensure that the top surface of the soilbag remains flat during the loading process. A uniform vertical displacement is applied to the loading panel over a number of increments. The width of the loading panel is sufficiently large so that the soilbag will not be squeezed out of the loading panel even after large deformation.

In the three-dimensional model, the bag and the soil are discretised into uniformly distributed elements. The soil is represented by 8-noded linear 3D elements (C3D8), whilst the bag by 4-noded quadrilateral membrane (M3D4) elements. The main characteristics associated with the plane stress membrane elements are the insignificant bending and transverse shear stiffness. The loading panel is assumed to be a rigid body and meshed accordingly. Fig. 2 illustrates the parts required in the assembly of a soilbag. In the 2D model, 4-node plane strain quadrilateral elements (CPE4) are used both for the soil and the bag. The elements for the soil are refined as approaching the soil-bag interface as shown in Fig. 1b. The elements for the bag are very fine, due to the small thickness (0.1 mm) of the bag.

For the problem presented, two distinct contact interfaces are defined to model the soil/bag and bag/loading panel interactions: the soil/bag interface is modelled using the surface-to-surface finite-sliding formulation with the concept of master surface (soil) and slave surface (bag), and the bag/loading panel interface is modelled via node-to-surface finite-sliding formulation using master (loading panel)/slave (bag) approach as formulated in ABAQUS. The master and slave surfaces are defined as shown in Fig. 3.

The elements in the soil and bag domain that are initially in contact are defined as interacting surfaces. However, for the loading panel/bag contact, those nodes with the possibility of contact during the analysis are selected as interacting node regions. This allows the possibility of elements on the bag surface coming into contact with the loading panel as the analysis progresses. For soil/bag contact interaction using a surface to surface discretisation method, an automatic smoothing is applied to contacting surfaces in order to reduce inaccuracies in contact pressures caused by mesh discretisation on curved geometries of a soilbag with lateral boundaries. Details of interacting surfaces are presented in Table 1.

The contact between the bag and the loading panel also follows the Coulomb friction law with a coefficient of friction of 0.5. In order to establish a uniform loading condition throughout the analysis, no surface separation is allowed during loading steps (see Table 2–4).

The numerical analysis is carried out in two individual steps. The first step of the analysis establishes the initial contacts between the loading panel and the bag and between the bag and the soil. The vertical compression is applied during the second step.

The soil is assumed weightless throughout the numerical simulation. The boundary conditions are shown in Fig. 3. Because the problem involves various nonlinearities (material, boundary conditions and large deformation), numerical convergence is a challenge and very fine time steps have to be used.

2.4. FE Mesh for soilbag under cyclic shearing

In this part, an 80 cm × 40 cm × 10 cm soilbag is subjected to cyclic simple shear and its mechanical behaviour is investigated through two- and three-dimensional numerical simulation. Assuming the mid-plane of the soilbag remains stationary during the shear test, we consider half of the soilbag. The geometry and finite element meshes are shown in Fig. 4. Mesh and element type assigned to the two- and three-dimensional model for this scenario is very similar to those of the case of a vertical compression (Fig. 2a), with the soil represented by 8-noded linear elements and bag by 4-noded membrane elements. Since the soil has a small dilation angle and its volume may increase to some extent during the shear test, quadratic elements are used here instead of linear elements. Quadratic elements are generally considered to be better

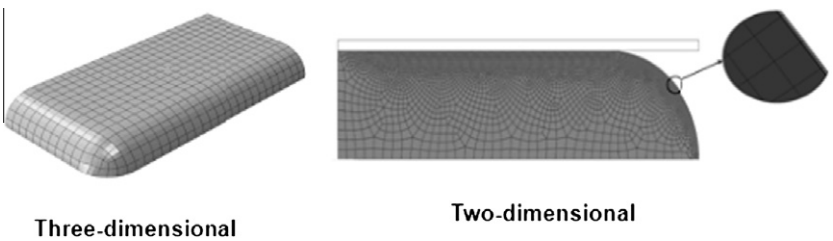

Fig. 1. Initial geometry and finite element mesh of the soilbag assembly.

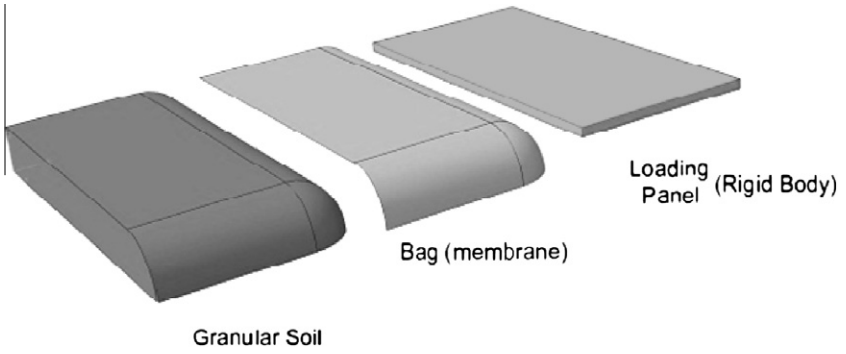

Fig. 2. Main parts for the assembly of a soilbag (3D model).

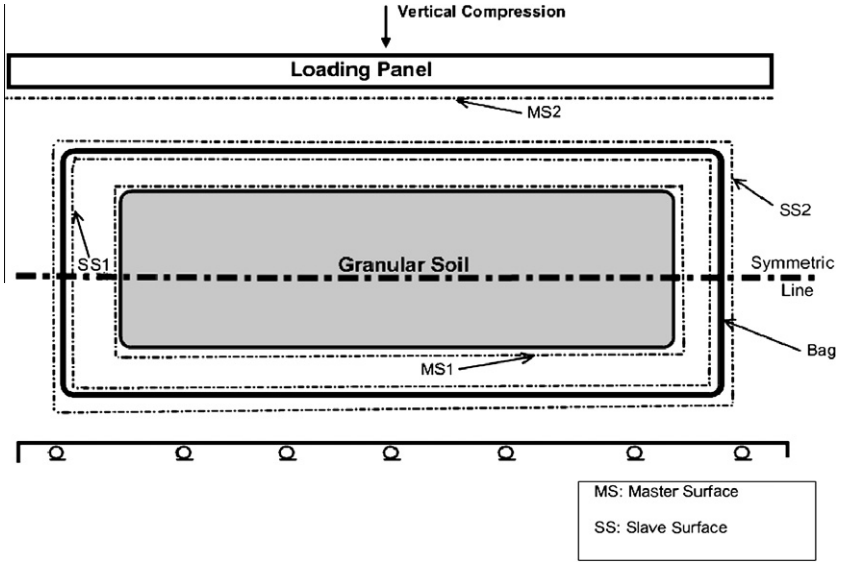

Fig. 3. Geometry and boundary conditions for the assemblage of soilbag.

Table 1
Polyethylene bag properties.

Bag	Value	Unit
Young's Modulus (E)	500	MPa
Yield Stress	100	MPa
Poisson's ratio (v)	0.3	–
Thickness	0.1	mm

Table 2
Soil properties.

Oil (sand)	Value	Unit
Young's modulus (E)	100	Mpa
Poisson's ratio (v)	0.3	
Cohesion	1	kPa
Friction angle	40	Degree
Dilation angle	5–15	Degree

Table 3
Soil-bag-loading panel interface properties.

Interface	Friction coefficient	Friction angle	Separation allowed
Soil-bag	0.84	38	Yes
Bag-loading panel	0.5	26	No

Table 4
Details of the surface interactions for the assembly of a soilbag.

Feature		
Interface	Soilbag	Bag-loading plate
Discretisation method	Surface to surface	Face to surface
Tracking approach	Finite sliding	Finite sliding
Constraint enforcement method	Penalty method	Penalty method
Surface smoothing	Yes	No

than linear elements for incompressible or dilatant materials, even though numerical tests for the problem studied here show very little difference in the results. Cyclic horizontal displacement is applied to the loading panel over a number of increments.

The analysis is carried out in three steps: the first step to establish the contact interactions between interfaces, the second step to apply a monotonic vertical compression on the load panel and the third step to apply cyclic horizontal displacements to the loading panel while the vertical load is maintained throughout the analysis. To ensure the shear is applied to the soilbag, a relatively high coefficient of friction between the loading panel and the bag ($\mu = 0.99$) is used.

The boundary conditions for the cyclic simple shear test are similar to those shown in Fig. 3, except that the horizontal movement at

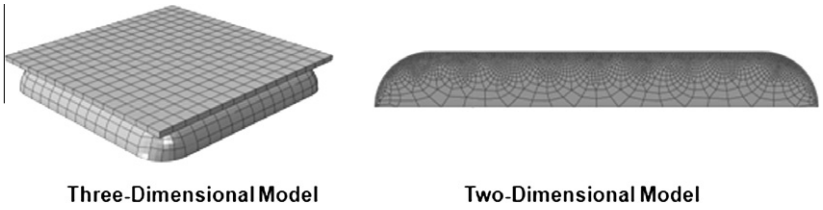

Fig. 4. Initial geometry and mesh of the assembly of a soilbag under cyclic shear.

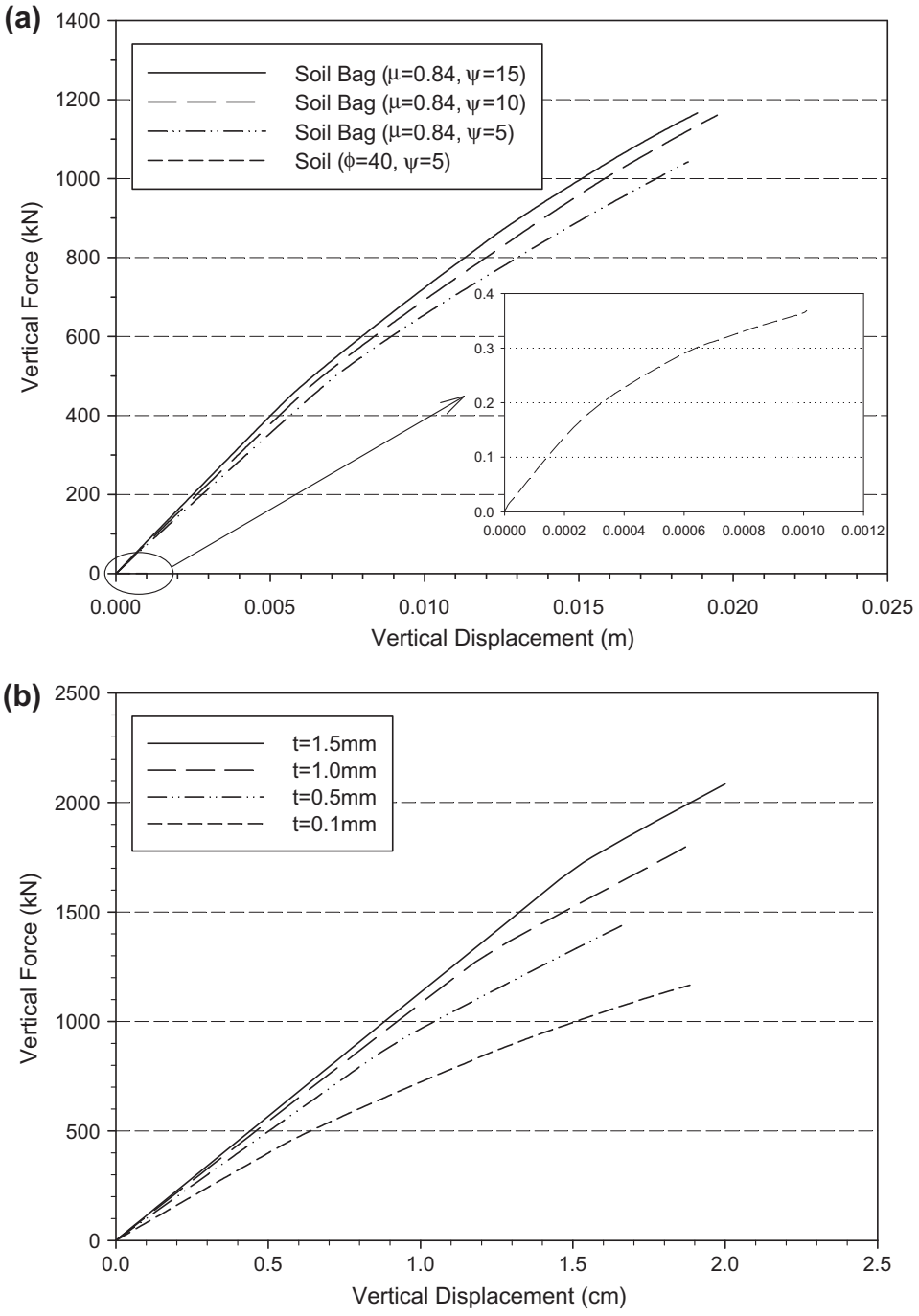

Fig. 5. Load–displacement relationship for a 3D assembly of soilbag under vertical compression for (a) different soil types, (b) various bag thicknesses.

the mid-plane (symmetric line in Fig. 3) is not allowed during the last step. A surface-to-surface finite sliding master/slave contact is chosen to define the soil/bag interface. In this simulation, a 'path-based' tracking algorithm has to be considered to model the membrane with double-sided contact surfaces. The 'path-based' tracking algorithm is the only algorithm that allows for

double-sided master/slave contact surfaces [1]. The automatic smoothing is also enabled due to the semi-circular boundaries of the soilbag.

3. Numerical results

3.1. Mechanical behaviour of a soilbag under vertical compression

The numerical load-settlement relationship of a three-dimensional soilbag experiencing unconfined compression for (a) different soil types, and (b) different bag thickness are illustrated in Fig. 5. As shown, a comparison between the compression behaviour of the granular material and the soilbag indicates a dramatic increase in the stiffness and the compression capacity of the assembly of soilbag (see Fig. 5).

Evolution of separation-reclosure of contact surfaces within a soilbag under vertical compression for a three-dimensional model is illustrated in Fig. 6. It should be noted that the distribution of these contact surfaces partially depends on the discretisation characteristics such as mesh dimension and element type. Two-dimensional numerical analysis of a soilbag subject to vertical compression load and cyclic simple shear load are also obtained which provide more convenient outputs to investigate local separation as well as evolution of stresses within the soilbag. Fig. 7 shows the evolution of the tensile force up to its limits within a bag with a thickness of 0.1 mm and a yield capacity of 100 MPa for a three-dimensional sandbag under vertical compression.

3.2. Comparison with analytical solution for a soilbag under vertical compression

An analytical solution to the problem of loading capacity of the sandbags under vertical compression is proposed in Matsuoka et al. [8] and Tantono and Bauer [23]. The analytical solution employed in here is similar to the solution of Tantono and Bauer [23] to evaluate the deformation characteristics of soilbags. This solution is briefly explained in the following.

In order to achieve an analytical solution, several simplifying assumption need to be introduced to the problem. Some of these assumptions include:

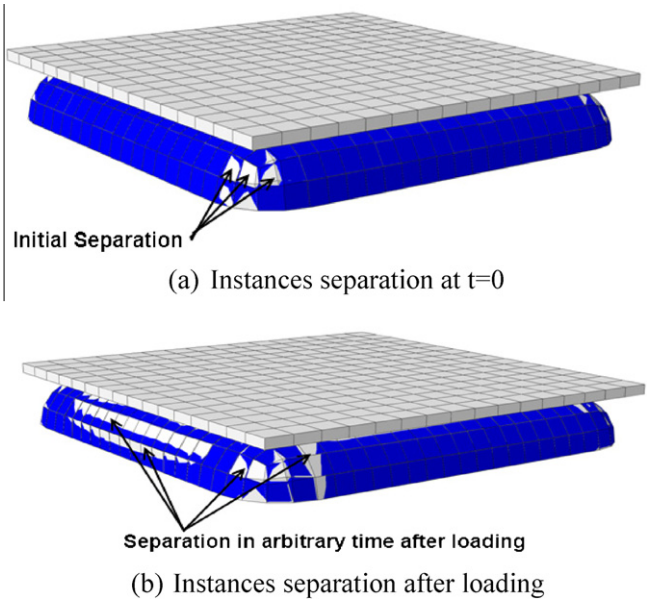

Fig. 6. Separations at the soil-bag interface (a) prior to, and (b) after compression loading.

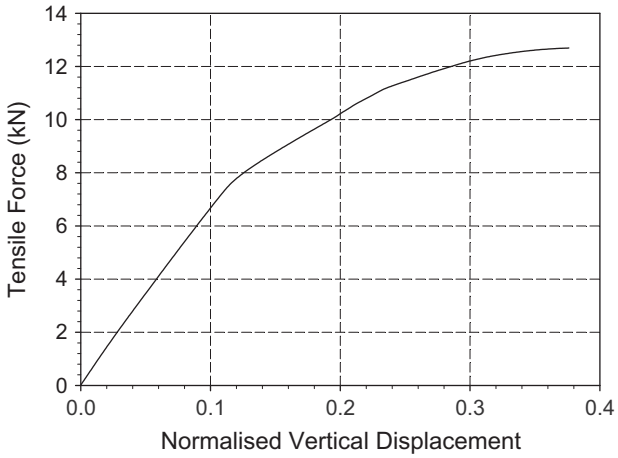

Fig. 7. Evolution of the tensile force within a bag during vertical compression.

1. Plane strain condition is considered.
2. The soilbag is totally filled with granular material.
3. The change within the bag thickness as a result of bag expansion under vertical loading is ignored.
4. Hypothetical distribution of different stress components are considered as shown in Fig. 8.
5. No lateral stress is introduced to the soilbag structure.
6. Frictional contacts between the soil-bag and the bag-loading panel interfaces are neglected.

The vertical compression associated with the yielding tensile strain within the bag could be derived via equilibrium equations in the horizontal and vertical directions (Fig. 8b and c) as expressed below:

$$\sum F_x = 0: \quad \sigma_h \times H - 2T \times l = 0 \tag{3}$$

$$\sum F_y = 0: \quad \sigma_v \times B \times l + 2 \times \sigma_v \times H \times l - 2T \times B \times l - f_v \times B \times l = 0 \tag{4}$$

where B and H are the width and height of a soilbag, respectively; l is the length of the bag; T is the bag tensile force; and subscript '0' represents the initial dimensions of a soilbag prior to loading.

The horizontal and vertical stresses can be linked via a passive earth pressure:

$$\sigma_v = K_p \cdot \sigma_h \tag{5}$$

where for a granular soil with friction angle of ϕ the passive earth pressure coefficient is given as:

$$K_p = \frac{1 + \sin\phi}{1 - \sin\phi} \tag{6}$$

In order to estimate the maximum vertical load which could be applied to a soilbag, the tensile force within the bag should be substituted by $T = (\sigma_y)_{bag} \times t_{bag}$.

For a soilbag with semi-circular boundaries, we have:

$$L_0 = 2B_0 + \pi H_0 \tag{7}$$

$$V_0 = B_0 \cdot H_0 \cdot l + \pi \times (H_0)^2 \cdot l \tag{8}$$

where L_0 and (V_0) are the initial perimeter and volume of that soilbag, respectively. Now, if the soilbag experiences a vertical deformation, δ_v, these components will change accordingly using the continuity equation:

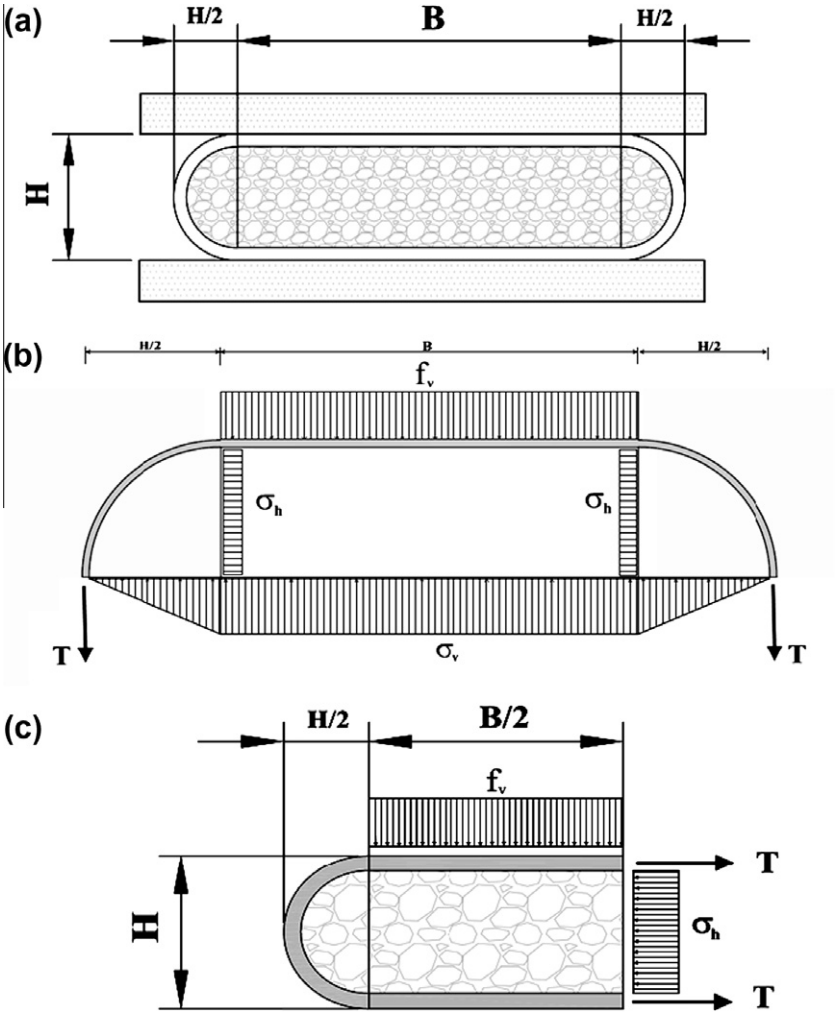

Fig. 8. (a) Geometry, (b) horizontal section, and (c) vertical section of a soilbag under vertical compression.

$$H = H_0 - \delta_v \tag{9}$$

$$V = V_0 \rightarrow B = \frac{B_0 H_0 - \frac{\pi H_0 \delta_v}{2} - \frac{\pi}{4(\delta_v)^2}}{(H_0 - \delta_v)} \tag{10}$$

$$L = \frac{2B_0 H_0 - \pi H_0 \delta_v + \frac{\pi \delta_v^2}{2} + \pi H_0^2}{(H_0 - \delta_v)} \tag{11}$$

The tensile strain of the bag can then be calculated as:

$$\epsilon_{bag} = \frac{L - L_0}{L_0} = \frac{\delta_v(\pi\delta_v + 4B_0)}{2(H_0 - \delta_v)(2B_0 + \pi H_0)} \tag{12}$$

The vertical displacement corresponding to the bag yield strain can then be derived by substituting the bag yield tensile strain with its limited value, $(\epsilon_y)_{bag}$:

$$\frac{\delta_v(\pi\delta_v + 4B_0)}{2(H_0 - \delta_v)(2B_0 + \pi H_0)} - \frac{(\sigma_y)_{bag}}{E} = 0 \tag{13}$$

Based on these analytical solutions it could be found that the maximum vertical displacement of a soilbag is not a function of the bag thickness. The compression capacity of a soilbag would be equal to:

$$F_{limit} = 2(\sigma_y)_{bag} \times t \times \left[\frac{B \cdot K_p}{H} + \frac{K_p}{2} - 1\right] \times l \tag{14}$$

Compression capacity of an $80 \times 40 \times 10$ cm soilbag under vertical compression is studied both numerically and analytically. A polyethylene bag with a thickness of 0.1 mm, a modulus of elasticity of 500 MPa, and a tensile yield stress of 100 MPa is modelled. The bag is filled with sand with a friction angle of 40°. Three-dimensional model is used for numerical analysis of this soilbag. Analytical results report a vertical bearing capacity of 1185.6 kN and a maximum vertical displacement of 19 mm for this case, whereas the numerical model gives respective values of 1252.5 kN and 15.4 mm.

Fig. 9a and b shows the variation of the vertical load capacity and maximum vertical deformation of this soilbag for a range of tensile yield stresses, respectively. As illustrated, both the compression and deformation capacities of this soilbag increase quite linearly in the analytical model with any increase in the yield stress of the bag. However, based on the numerical results, the vertical compression capacity and maximum vertical deformation of soilbags are found to reach a plateau for higher tensile strengths. This difference is mainly a result of simplifications inherent within the analytical solution. It should be borne in mind that the analytical solution is principally based on the yield tensile strength of a bag while the numerical results indicate that the load capacity of sandbags are highly proportional to the stiffness parameters and shear strength of the filling materials.

The effect of the bag thickness on the compression capacity and deformation capacity of soilbags is also investigated. Fig. 10a and b illustrates the variation of these parameters with the bag thickness. According to Eq. (14), the compression capacity of this soilbag

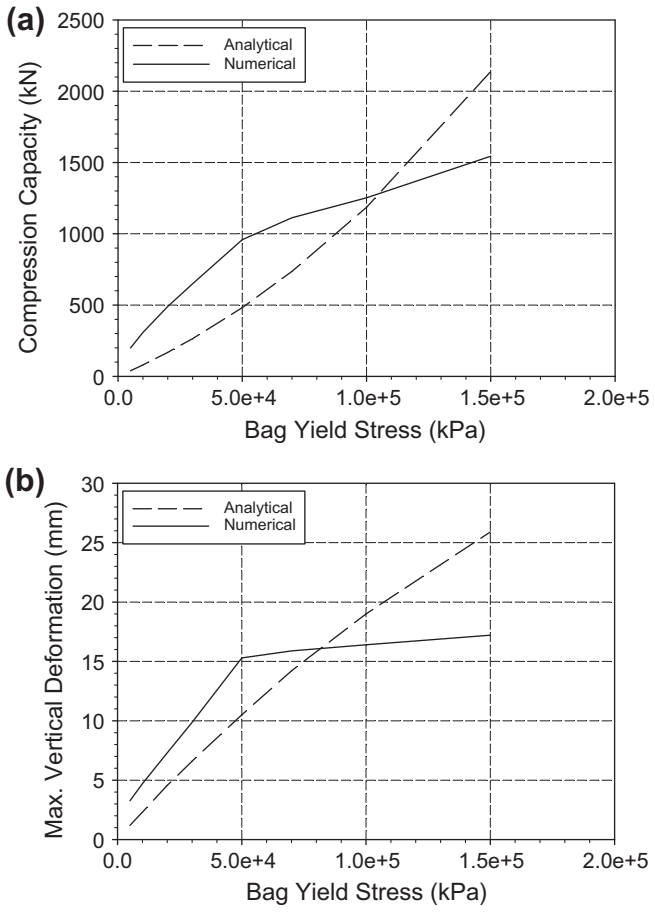

Fig. 9. (a) Vertical compression capacity and (b) maximum vertical deformation of an 80 × 80 × 10 cm soilbag under vertical compression.

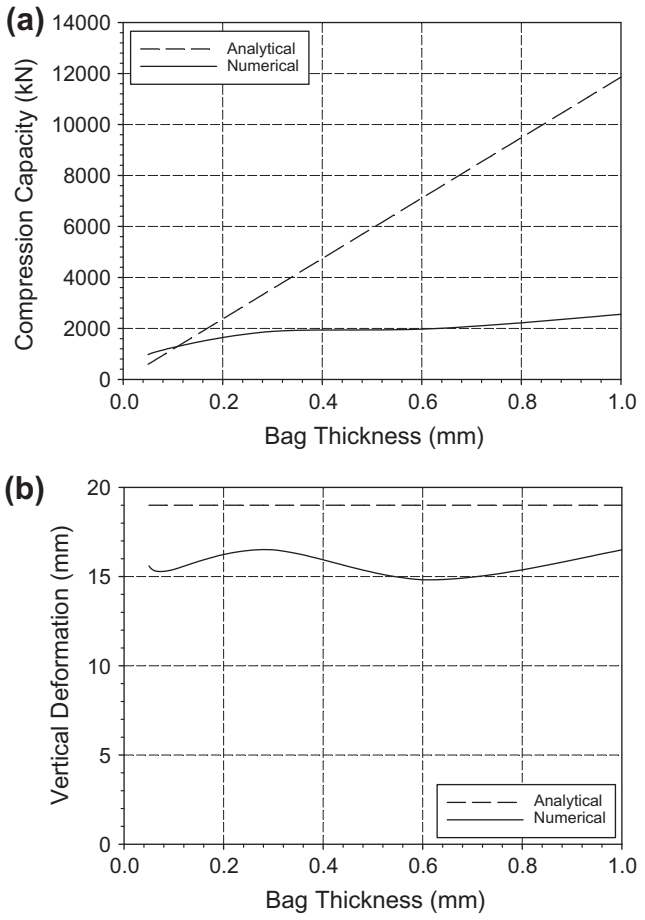

Fig. 10. Variation of (a) compression capacity and (b) deformation capacity of a soilbag under vertical compression for an 80 × 80 × 10 cm soilbag.

would increase linearly with the thickness of the bag, but the numerical results show a completely different trend due to the assumptions inherent within the simplified analytical model as discussed previously. The numerical compression capacity is significantly less sensitive to the bag thickness. On the other hand, both analytical and numerical results demonstrate similar independency of the maximum vertical deformation of soilbags to the bag thickness as plotted in Fig. 10b. It should be noted that most commercially-produced bags have thicknesses ranging between 0.1 and 0.7 mm.

3.3. Mechanical behaviour of a soilbag under cyclic shear test

The numerical horizontal load–displacement relationship of a soilbag undergoing cyclic shear is shown in Fig. 11. Local separation at the soil-bag interface during an arbitrary cyclic shear test is illustrated in Fig. 12.

Application of soilbags as vibration-reducing structural elements necessitates a study on the energy absorption potential within a soilbag throughout a cyclic simple shear test. The energy balance equation of the entire soilbag under cyclic shear test can be written as:

$$E_I + E_V + E_{FD} - E_W = E_{total} = \text{constant} \tag{15}$$

and,

$$E_I = E_E + E_{PD} + E_{VE} \tag{16}$$

where E_I is the internal energy; E_V and E_{FD} define the energies dissipated by damping and frictional contact mechanisms, respectively; E_W is the work done by the externally applied loads; and E_E , E_{PD}, and E_{VE} represent elastic dissipated strain energy, inelastic dissipated energy, and visco-elasticity dissipated energy, respectively.

The evolution of the different energy components in a soilbag assembly (with the friction coefficient of 0.84) while subjected to a cyclic shear test is presented in Fig. 13. Evolution of frictional dissipation (E_{FD}) defines the fraction of the frictional work mainly converted to heat among contacting surfaces. Heat is instantaneously distributed among each of the contacting bodies by conduction and radiation since no heat capacity is considered for the contact interface.

In the coupled thermal–mechanical surface interactions, the rate of frictional energy dissipation is given by:

$$P_{fr} = \tau_{cr} \cdot \dot{\gamma} \tag{17}$$

and

$$\tau_{cr} = \sqrt{\tau_1^2 + \tau_2^2} \tag{18}$$

where τ_{cr} is the critical frictional stress, τ_1 and τ_2 are active shear stresses on the contacting surface, and $\dot{\gamma}$ is the slip rate. The portion of this energy released as heat on master surface A and slave surface B would be:

$$E_{FD(A)} = f \cdot \eta \cdot P_{fr} \quad \text{and} \quad E_{FD(B)} = (1-f) \cdot \eta \cdot P_{fr} \tag{19}$$

where η is the fraction of dissipated energy converted to heat (ABAQUS default value is 1.0), and f is the weighting factor which defines the distribution of heat between contacting bodies (= 0.5). Fig. 14 shows the numerical results of the evolution of E_{FD} inside a sandbag

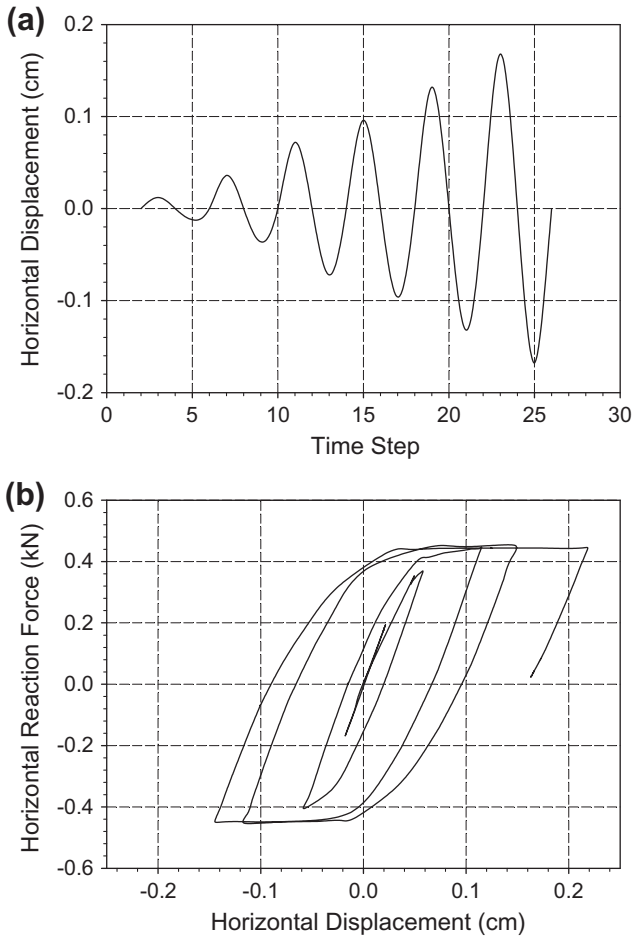

Fig. 11. (a) Horizontal displacement, and (b) typical hysteretic load–displacement curves for a 3D soilbag under cyclic shear.

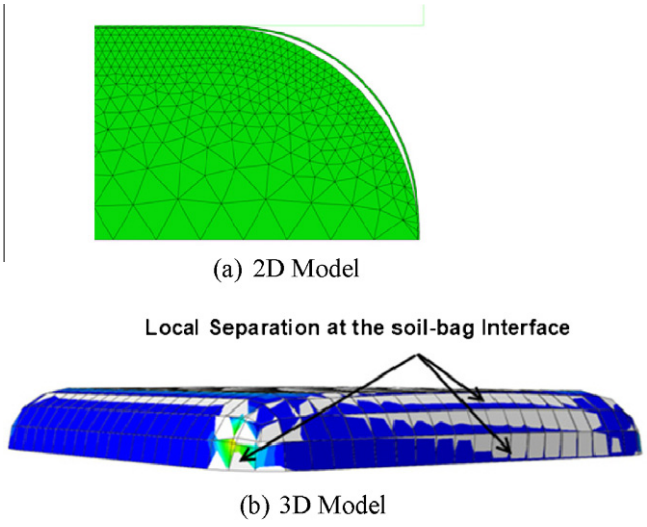

Fig. 12. Local separation-reclosure at the soil-bag interface during the cyclic shear test.

for different friction coefficients between soil and bag interface. As illustrated, E_{FD} increases with decreasing value of friction coefficient (μ) as a result of the increase in the slip rate ($\dot{\gamma}$). Conversely, the inelastic dissipation energy of a soilbag assembly demonstrates a completely different trend with any increase in the value of μ (Fig. 14b).

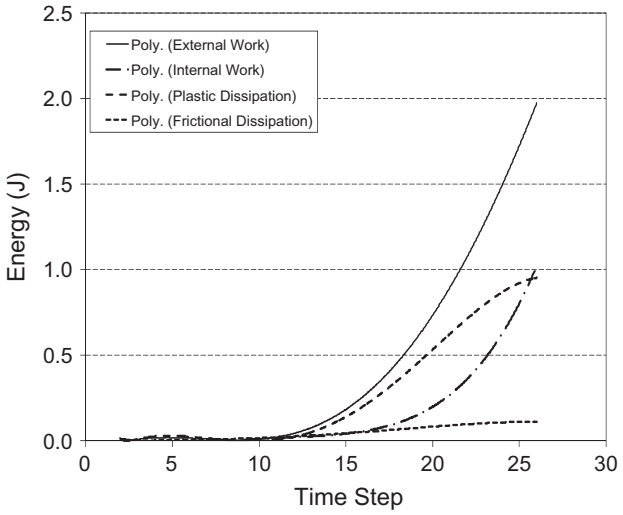

Fig. 13. Evolution of energy components within a soilbag during cyclic shear test.

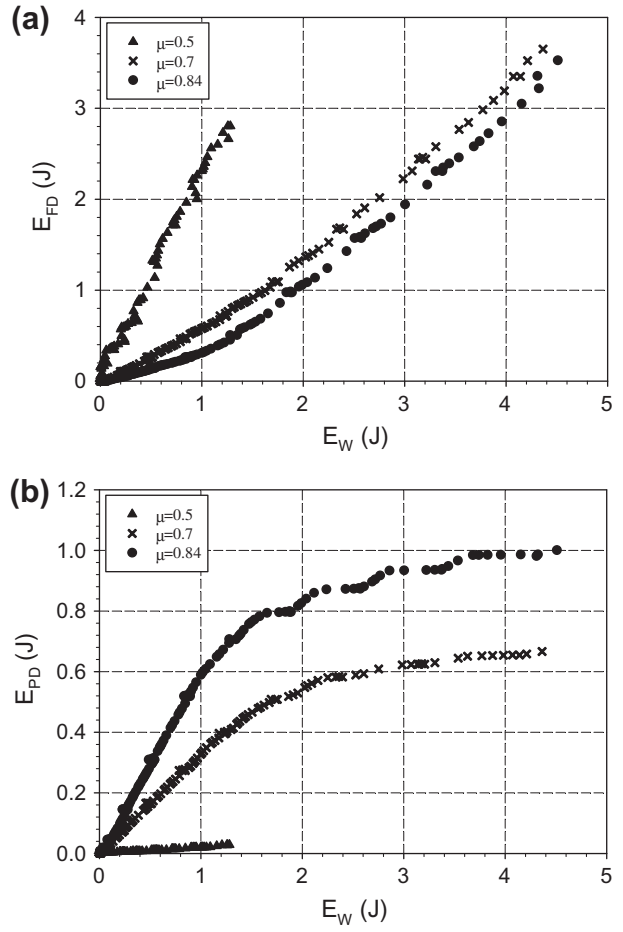

Fig. 14. Variation of energy components (a) E_{FD} vs E_w, and (b) E_{pd} vs E_w for a soilbag assembly under cyclic loading.

It is noticeable that the inelastic component of the energy, E_{PD}, under cyclic loading would increase with any particular increase in the tangential friction of the soil-bag interface while predictably, the frictional part of the total-dissipated energy would decrease with similar variation in the frictional coefficient μ. However, as illustrated in Fig. 15, the evolution of the totally-dissipated energy of a soil-bag assemblage ($E_{PD} + E_{FD}$) under cyclic loading is

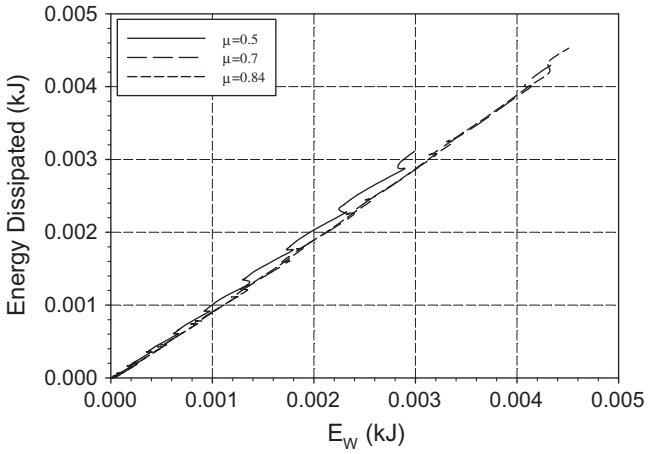

Fig. 15. Evolution of total-dissipated energy of a soilbag under cyclic shear.

somewhat linear while its magnitude is rather independent of the value of friction coefficient of a soil-bag interface.

4. Conclusions

The mechanical behaviour of the assembly of a soilbag subject to vertical (compression) loading and horizontal cyclic shear loading has been studied numerically using FE analyses. Unlike previous studies, the current work has specifically taken into account the active contact kinematic constraints at the soil-bag interface. This presents significant FE modelling challenges but is essential if the real behaviour of a soilbag is to be captured. Large-deformation frictional contact between the granular material (sand) and the wrapping material (bag) is modelled using the master surface/slave surface penalty method formulation. Two and three-dimensional models are presented in order to simulate the assemblage of the soilbag using the commercial finite element code 'ABAQUS' for its practical 3D mesh generation algorithms as well as its computational efficiency throughout large deformation contact mechanics simulations. To overcome the convergence difficulty, special care has been taken to ensure appropriate model discretisation and element type selection, and to ensure mesh dimensions as well as contact discretisation are adequate (Table 1).

The current study has shown that the stiffness and compression capacity of a soilbag assembly is considerably higher than an unwrapped granular material. Although previously presented analytical solutions are reasonable at approximating the deformation capacity of a soilbag under vertical compression, prediction of compressive load capacity of soilbags via these analytical solutions produces significant errors. Technically, these methods contain various simplifying assumptions such as neglecting the soil-bag interactions during vertical compression.

A brief study on the evolution of different energy components within the structure of a sandbag under horizontal cyclic loading indicated that though the magnitude of different energy components vary with the friction coefficient of a soil-bag interface, the variation of the total-dissipated energy with respect to the soil-bag friction angle is rather insignificant.

The work presented represents an initial attempt to model a very complex geotechnical problem. A comparison with previously published laboratory and analytical solutions for sandbags shows encouraging agreement. Accordingly, further investigation is planned to facilitate analysis of the structures constructed with soilbags.

References

[1] ABAQUS/standard user's manual. Version 6.7, Hibbitt, Karlsson & Sorensen; 2001.
[2] Argyris J, Faust G, Szimmat J, Warnke EP, William KJ. Recent developments in the finite element analysis of PCRV. In: 2nd int conf SMIRT, nuclear engineering and design, Berlin; 1974. p. 42–75.
[3] Kubo T, Yokota Y, Ito S, Matsuoka H, Liu, SH. Trial construction and behaviors of an arching structure with large-sized soilbags. In: Proceedings of the 36th Japan national conference on geotechnical engineering; 2001. p. 2099–100.
[4] Lade PV, Duncan JM. Elastoplastic stress–strain theory for cohesionless soil. Geotech Eng Div ASCE 1975;101:1037–53.
[5] Lambe TW, Whitman RV. Soil mechanics. New York: Wiley; 1979.
[6] Lohani TN, Matsushima K, Aqil U, Mohri Y, Tatsuoka F. Evaluating the strength and deformation characteristics of a soil bag pile from full-scale laboratory tests. Geosynth Int 2006;13(6):246–64.
[7] Matsuoka H. Tribology in soilbag. J Jpn Soc Tribol 2003;48(7):547–52.
[8] Matsuoka H, Hasebe T, Liu SH, Shimao R. Friction property of soilbags and some measures to increase soil bag resistances against sliding. In: Proceedings of the 38th annual symposium on geotechnical engineering, Akita, Japan; 2003. p. 869–70.
[9] Matsuoka H, Liu S. A new earth reinforcement method using soilbags. London: Taylor & Francis; 2006.
[10] Matsuoka H, Liu SH. New earth reinforcement method by soilbags ("donow"). Soils Found 2003;43(6):173–88.
[11] Matsuoka H, Liu SH, Yamaguchi K. Mechanical properties of soilbags and their application to earth reinforcement. In: Proceedings of the international symposium on earth reinforcement, Fukuoka, Japan; 2001. p. 587–92.
[12] Matsuoka H, Nakai T. Stress-deformation and strength characteristics of soil under three different principal stresses. Proc JSCE 1974:59–74.
[13] Matsushima K, Aqil U, Mohri Y, Tatsuoka F. Shear strength and deformation characteristics of geosynthetic soil bags stacked horizontally and inclined. Geosynth Int 2008;15(2):119–35.
[14] Merifield R, White DJ, Randolph MF. The ultimate undrained resistance of partially embedded pipelines. Géotechnique 2008;58(6):461–70.
[15] Muramatsu D, Zhang F, Shahin HM. Numerical simulation on bearing capacity of soilbag-reinforced ground considering finite deformation. Jpn Geotech J 2007;2(1):11–23.
[16] Muramatsu M, Bin Y, Zhang F. Numerical simulation of vibration damping effect of soilbag. Jpn Geotech J 2009;4(1):71–80.
[17] Nakai T, Hinokio M. A simple elastoplastic model for normally and over consolidated soils with unified material parameters. Soils Found 2004;44:53–70.
[18] Sheng D, Eigenbrod KD, Wriggers P. Finite element analysis of pile installation using large-slip frictional contact. Comput Geotech 2005;32(1):17–26.
[19] Sheng D, Sloan SW. of finite element implementation of critical state models. Comput Mech 2000;2(26):185–96.
[20] Sheng D, Sun DA, Matsuoka H. Cantilever sheet-pile wall modelled by frictional contact. Soils Found 2006;46(1).
[21] Sheng D, Wriggers P, Sloan SW. Application of frictional contact in geotechnical engineering. Int J Geomech 2007;7(3):176–85.
[22] Suzuki T, Yamashita S, Matsuoka H, Yamaguchi K. Effect of wrapped gravel on prevention of frost heaving. In: The 35th Japan national conference on geotechnical engineering, Japan; 2000. p. 609–10.
[23] Tantono SF, Bauer E. Numerical simulation of a soilbag under vertical compression. In: The 12th international conference of International Association for Computer Methods and Advances in Geomechanics (IACMAG), Goa, India; 2008.
[24] Tatsuoka F, Tateyama M, Uchimura T, Koseki J. Geosynthetic-reinforced soil retaining walls as important permanent structures. Geosynth Int 1997;4(2):81–136.
[25] Wriggers P. Computational contact mechanics. Berlin, Heidelberg: Wiley & Sons; 2002.
[26] Yamamoto H, Matsuoka H, Simao R, Hasebe T, Hattori M. Cyclic Shear Property and damping ratio of soilbag assembly. In: Proceedings of the 38th Japan national conference on geotechnical engineering; 2003. p. 757–8.